STREAMLINED LENS-RADOMES

Alan F. Kay

TECHNICAL RESEARCH GROUP

The conventional antenna used with a radome is a paraboloidal dish and feed. The feed serves as a source of spherical waves and the dish focuses or collimates this energy into locally plane waves which travel out into space. The function of the radome in this process is to act as if it were not there. A focusing element of another type occasionally used instead of the dish is a dielectric lens. At the same time the lens action of radomes with intentional or unintentional tapers has frequently been observed. It seems natural to ask if it is not possible to combine the function of the dielectric housing, the radome, and the antenna focusing element into a single unit, a "lens-radome".

In a certain sense, "lens-radomes" have been used before. Any time a dielectric lens is used in a flush mounted application or without a radome, the focusing and housing functions are being performed by a single component. But such applications are not the ones in which radomes have difficult problems. For one thing, until now lens-radomes have not been streamlined. Their exterior surfaces have been flat, almost flat, or at most, spherical.

An example of the latter, which we will refer to a number of times again, is the Luneberg lens. Let me recall (Slide 1) that a Luneberg lens is a spherically symmetric lens whose index of refraction (which is the square root of the relative dielectric constant) varies radially from a maximum of $\sqrt{2}$ at the center to a value unity on the outer surface following the law $n^2 = 2 - (r/a)^2$, where a is the radius. On the basis of geometrical optics, a point source placed on the surface of the Luneberg lens focuses into a plane collimated beam. Because of the spherical symmetry, the beam will scan throughout all space without distortion if the source traverses the surface of the lens appropriately.

Lunebergs have been built and tested at many laboratories and have been found to operate well in the microwave range up to frequencies above X band. Some of you who have had so little luck with geometrical optics in radome error analysis, may be skeptical of a purely optical design working so well in this case. A proof that geometrical and physical optics are quite accurate for the Luneberg lens has been obtained by Henry Jasik, who in his doctoral thesis at P.I.B. gave an exact electromagnetic solution of radiation from both a dipole and an omnidirectional source on the surface of a Luneberg lens. Jasik compared this solution with the physical optics solution and found no practical difference for the main lobe and the first side lobes for the case of a lens as small as 2 1/2 wavelengths in diameter. Unlike conventional radomes a Luneberg lens has a slowly varying refractive index. There are no index discontinuities and the maximum index value is relatively small.

The reason I have spent a little time talking about the Luneberg lens is that I want to describe today designs for streamlined lens-radomes of which the Luneberg lens is a special non-streamlined-case. Before doing so, I would like to discuss briefly the preliminary considerations which led us to this design. To begin with, our ultimate goal has been an axially symmetric dielectric lens-radome, with fineness ratios as high as 3 to 1, capable of scanning to $\pm 45^{\circ}$, and usable in applications where there are weight, strength, thermal and erosion problems, as well as electrical transmission and boresighting requirements.

Certain theoretical considerations, as well as the weight of experience, shows that only the Luneberg lens and certain modifications of the Luneberg which are also spherically symmetrical can achieve perfect focusing for a range of scan angles. We thus consider designs which focus approximately throughout a scanning range. We have restricted our attention primarily to a two dimensional analysis in the plane of the feed offset. Considerations under this two dimensional restriction are sufficient to show that most design approaches are unsatisfactory. A number of design procedures were considered at first. These utilized homogeneous, multilayered, and continuously varying indices. The continuously varying indices included radial variation, linear variation both axial and transverse, and combinations of all of these. In every case, a particular type of index variation was considered first, then some criterion of focusing and scanning was employed such as two or three point correction or the Abbé sine condition, and then the ray paths were determined. Let me call this the "analytical" approach. These attempts were abandoned for one or more of the following reasons: inadequate streamlining, computational complexity, inadequate scanning range, or impractical index values.

The design which has proved most successful and which I shall discuss today reverses the analysis procedure. We start by choosing a field of curves which, if they were rays, would mean good focusing and scanning properties. Then we "synthesize" a variable refractive index such that the rays associated with this index are the chosen curves. We thereby realize the desirable focusing and scanning properties.

Let me illustrate this method with an example (Slide 2). Suppose we would like the outer surface of the lens-radome to be an ellipse given by equation (1) where the source, or feed phase center, is at the point (-1,0). Observe that for A sufficiently large, the fineness ratio is as large as you please. Now we want a family of rays which focus and imply some scanning ability. We choose the family of ellipses specified by a parameter t in equation (2), where θ is the angle that the ray makes with the axis at the source. These curves were chosen for a number of reasons:

(1) they focus, that is they all start from the axial feed point and emerge at the outer surface of the lens parallel to the axis.

(2) they satisfy the Abbé sine condition. This condition

implies that when the feed point is moved off the axis for a short distance the beam will scan and the lens will continue to focus, not only those rays in the plane shown, but also the rays leaving the source and entering the lens in all directions in space.

3) When A = 1, this design reduces to the ordinary Luneberg lens. By taking A larger than 1, we are thus, in a way, "pushing out" the Luneberg lens, proceeding from the known to the unknown - and since A is arbitrary - with as big a jump as we care to take.

Now how do we determine a refractive index variation which actually makes the curves of equation (2) into rays? We have the differential equation (3) of a ray in a continuously varying medium, which says that the ray's curvature $\varkappa$ equals the dot product of the unit normal to the ray $\bar{n}$ and the gradient of the logarithm of the refractive index. This equation is a direct consequence of the eikonal equation (4) for the wave fronts, ψ = constant. The eikonal equation may be derived as the asymptotic solution of Maxwell's equations for the phase of the field as $\lambda \to 0$. Both of these derivations are given in Silver's antenna book. From the equations of the rays we can find expressions for their unit normals and their curvature. In an analysis design one would have the index and a desire to find the ray paths. Here we have the ray paths and desire the index n(x,y). This requires solving a first order partial differential equation - which can be done by the following method. We first find the orthogonal trajectories of the rays; these are the wave fronts. This can be done by numerically integrating the first order ordinary differential equation (5), or by the simple graphical means of starting at a point on the outer lens surface and, with the aid of triangles, tracing by eye a curve which intersects each successive ray at right angles. The graphical method has been quick, simple, and accurate for this problem.

Now if s is arc length along a particular wave front, then the ray equation may be integrated to yield equation (6). Upon substitution for curvature and changing the integration variable to t, we obtain (7) in which the integrand is a function of t alone by substitution of Θ from the solution of (5). In the Luneberg case (A = 1), these integrals may be found explicitly and we "rediscover" the Luneberg index variation. For the case A > 1, a numerical solution is required. Again a graphical procedure works well. We take a pair of dividers with a fixed small spacing Δ s, and lay off a series of equidistant points, say 1,2,..., j, on the wave front, the first point being at the outer surface. Then by the trapezoidal rule, applied to (6), the value of log n at the j-th point is found from equation (8) where $\varkappa_i$ is obtained by interpolation, from the values of curvature of the rays near the ith point. n_o is an arbitrary initial value of n (one of the nice points in this method is that the index on the outer surface is arbitrary). In this way, we determine n on each wave front and repeating for all the wave fronts we have n at a set of points covering the whole lens. By interpolation we determine contours

of constant index n, the "isofracts". This method was tested with the Luneberg lens, (case A = 1 in equation (2), and it gave the Luneberg index variation with an accuracy in n of ± .005 or better.

The results of this method for the case A = 2 are shown in Slide 4. Eight rays, fourteen wave fronts, and the isofracts in steps of .02 from 1.00 to 1.38 are shown. The lower half of the lens is symmetrical and is not shown.

As an illustration of a more streamlined case, rather than choose a larger value of A, we decided to employ a more practical, ogival outershape (Slide 5). Here the equation of the outer surface is given by (9). The equations of the rays are shown in (10). The case n_o = 1, is shown in Slide 6.

Since in actual fabrication the outer surface would probably be taken along the n = 1.02 isofract, the overall fineness ratio of such a lens radome would be about 2:1. If the index of the outer surface n_o is chosen greater than unity, then a refraction will take place at the boundary which must be accounted for in the equations for the rays. While our method still applies in principal, difficulty is experienced near the nose and a situation prevails which may be summarized as follows. In view of the requirements of focusing, the Abbé sine condition, and a large fineness ratio, if we ask for an index at the outer surface of n_o = 1.2 or greater, then the thickness through which an index appreciably greater than unity prevails, turns out to be so thin that it seems just as satisfactory and much simpler to work with an n_o = unity design to begin with and then add a thin high index layer to the outer surface. The error introduced thereby may be partially compensated for later.

Let us turn now to some practical considerations. How would one make such a variable index lens? To answer this question we examine the technology developed for the Luneberg and other variable index lenses. Let us consider a lens suitable for X band or lower frequencies. It has been found satisfactory to approximate the index gradient by ten homogeneous layers with index of refraction starting at 1.02 and increasing in steps of .04 with a tolerance of ± .01 or perhaps ± .02. Loss tangent must be less than .01 but dimensional tolerances are half the thickness of the layer and are no problem at all. Luneberg lenses are now available commercially from at least three places: Emerson and Cummings, Delaware Research and Development Corporation, and Scientific Associates, Inc. Their methods of manufacture differ. The layers may be machined or molded in matched dies. They may be made of polyfoam of various densities, perhaps loaded with conducting particles, or of a ceramic foam. They may be artificial dielectric.

All these techniques apply equally well to the streamlined lens-radomes. As an illustration of cost, it is estimated that a single experimental model of either the blunt or streamlined shape, held to tolerances and made by machining would cost $7,000. If matched dies were used, the cost would be much higher, especially since the layers are not spherical.

Two practical problems are transmission loss and weight. Table II shows the estimated maximum transverse diameter in wavelengths for a streamlined lens-radome for a 3 db and a 1 db maximum transmission loss for three typical materials. Table II also gives the weight of the lens-radome for two diameters and the same materials. The data indicates that loaded materials are likely to be far too lossy but that unloaded materials may be too heavy. Or, alternatively, a small lens-radome should have no loss or weight problem, but a large lens-radome would probably require an unusually low loss, light weight foam to be feasible. The ceramic foam, of course, has a thermal advantage, and it has been suggested that at least the outer shell might be made of ceramic for this reason.

Feeding the lens is another problem. Table III shows the maximum feed aperture diameter versus the lens radius. This data is based on physical optics and the Raleigh criterion.

The Abbé sine condition does not guarantee a large amount of scanning. How do these lenses behave off axis? Can they scan to 45°? To answer these questions, ripple tank model studies were made for TRG by H. D. Rix of the Pennsylvania State University Physics Department. To make the models we machined flat plexiglass stock on one side to a thickness predetermined so that when these models sat on the plate glass bottom of the ripple tank, and water covered them to the right depth, the velocity of 12 cps ripples over any point on the lens relative to that over "deep water" equaled the design refractive index of the lens at that point. The ripples were photographed by transmitted light, focused by the ripples themselves and frozen by a stroboscopic chopper driven synchronously with the source oscillator.

As a test of the validity of the ripple tank analogy for this particular problem, a 10 inch diameter model of a Luneberg lens was made and tested. Slide 8 shows the results with a point source. The emergent wave front is plane but with an amplitude oscillation having a 1λ period and believed to be an inherent diffraction effect. Slides 9 and 10 show a line source. The fine focusing properties of the Luneberg lens are clearly brought out.

One of the drawbacks of the ripple tank method is that attenuation can not be properly modeled. The ripple attenuation always exceeds that of a low loss dielectric especially when the index is high. Values above 1.5 can not be realized on the present Penn State ripple tank for this reason. In order to minimize this effect the streamlined models were made smaller, 10 cms. in transverse diameter.

Another difficulty is that the optical index of refraction of the plexiglass and the water differ so that over the non-flat portion of the lens, optical refraction errors distort the outlines of the lens and the wave fronts above. The ripples themselves distort smooth curves such as the lens boundary or machining lines so that their images appear cycloidal.

The next two slides show the blunt and streamlined lens-radomes, each 5λ in transverse diameter. At normal incidence focusing is as good as the Luneberg lens. The amplitude oscillations of period 1λ are still present in the emergent wave front. The next slide shows a tolerance study. The wave fronts behind are the ones on the previous slide. Those slightly ahead were photographed in a double exposure when the water depth was increased .17 mms so that the indices are related as shown. The next two slides show the blunt and streamlined lenses with the point source at about 30° off axis. The streamlined case is shown again in the next slide as a double exposure. The circular wave fronts of the source alone are shown superposed. The next slide shows the streamlined lens at 40° off axis. Definite beam deterioration is noticeable.

A line source properly models an incident field on reception. But since antenna feeds are not isotropic, a point source does not model the antenna properly on transmission. For this reason the line source photographs shown next are perhaps of more interest. We have the blunt lens at 0°, 15°, 30°, 40°, 50°, and 60° incidence, and the streamlined lens at 0°, 15° and 30°, incidence. Although we observe that the scanning range appears to be at least ± 30°, this study is still in progress and definite conclusions can not be stated at this time.

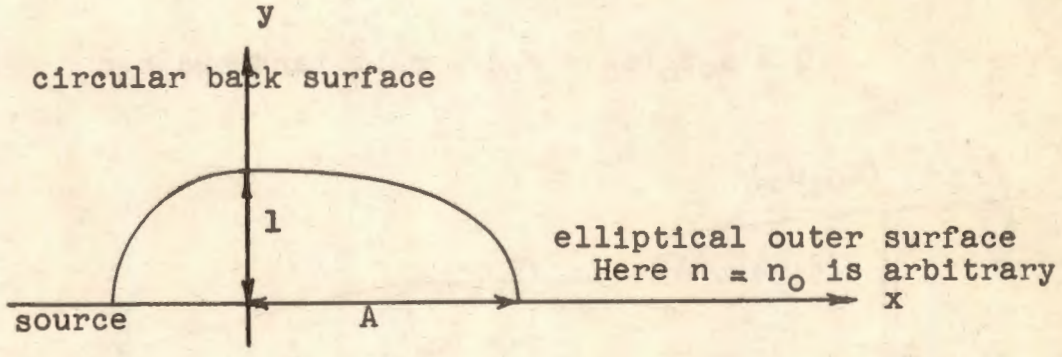

(1) $\left(\frac{x}{A}\right)^2 + y^2 = 1$

(2) $x = a \cos t + b \sin t + c$

$y = d \sin t \qquad 0 < t < \pi/2$

where

$a = (1 - A)\cdot\cos\theta - A \qquad b = \cos\theta$

$c = (A - 1)\cdot\cos\theta \qquad d = \sin\theta$

(3) $\kappa = \bar{n} \nabla \log n \qquad n = n(x,y)$

(4) $|\nabla \Psi|^2 = n^2$

(5) $$\frac{d\theta}{dt} = -\frac{y_t^2 + x_t^2}{y_t y_\theta + x_t x_\theta}$$

(6) $$\log n = \int \varkappa \, \partial s$$

(7) $$n(x,y) = n_o \exp \int_t^{\alpha} \frac{(y_t x_{tt} - x_t y_{tt})(x_\theta y_t - y_\theta x_t)dt}{(x_t^2 + y_t^2)(y_t y_\theta + x_t x_\theta)}$$

(8) $$\log n_j = \log n_o + \Delta s \left(\sum_{i=2}^{j-1} \varkappa_i + \frac{\varkappa_o + \varkappa_j}{2} \right)$$

(9) $$M(x^2 + y^2) + Nx + Py + Q = 0$$

where $M = b_o + (a_o - c_o) \tan \varphi$

$N = (b_o^2 + c_o^2 - a_o^2) \tan\varphi - 2a_o b_o$

$P = 2b_o(c_o - a_o) \tan\varphi + a_o^2 - b_o^2 + c_o^2 - 2a_o c_o$

$Q = a_o c_o (a_o - c_o) - c_o b_o^2 \tan\varphi + 2a_o b_o c_o - b_o c_o^2$

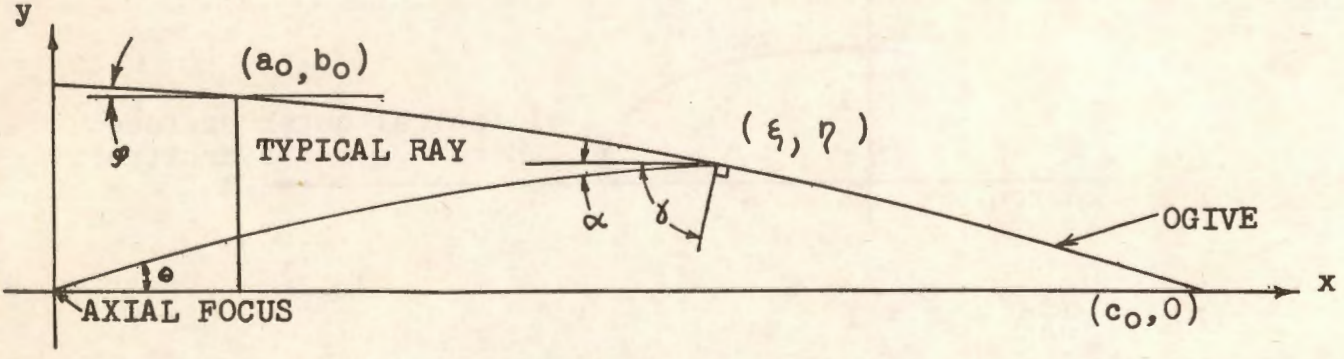

(10) $$Ax^2 + By^2 + Cx + Dy = 0$$

where $A = -\eta^2 \tan\theta$ $\qquad C = 2\xi\eta^2 \tan\theta$

$B = 2\xi\eta - \xi^2 \tan\theta$ $\qquad D = -2\xi\eta^2$

Table II

Material	Maximum diameter in wavelengths		Weight, lbs	
	for 3db loss	for 1db loss	diameter 5 inches	diameter 30 inches
1) Polystyrene foam	444	148	.89	193
2) Loaded polyfoam	6.3	2.1	.22	48.4
3) Ceramic foam	133	44	.71	154

Table III

Lens Radius in Wavelengths	Maximum Feed Diameter in Wavelengths (Raleigh Criterion)	
	$\lambda/8$	$\lambda/16$
3	.58	.33
4.8	.845	.483
6	1.0	.58
10	1.45	.87
18	2.16	1.34
30	3.0	1.92
50	4.1	2.68